ChemPubSoc Europe

Check for updates

N-Heterocyclic Olefins

N-Heterocyclic Olefins as Electron Donors in Combination with Triarylborane Acceptors: Synthesis, Optical and Electronic Properties of D–π–A Compounds

Jiang He, Florian Rauch, Alexandra Friedrich, Daniel Sieh, Tatjana Ribbeck,
Ivo Krummenacher, Holger Braunschweig, Maik Finze,* and Todd B. Marder*[a]

Abstract: N-heterocyclic olefins (NHOs), relatives of N-heterocyclic carbenes (NHCs), exhibit high nucleophilicity and soft Lewis basic character. To investigate their π-electron donating ability, NHOs were attached to triarylborane π-acceptors (A) giving donor (D)–π–A compounds **1**–**3**. In addition, an enamine π-donor analogue (**4**) was synthesized for comparison. UV–visible absorption studies show a larger red shift for the NHO-containing boranes than for the enamine analogue, a relative of cyclic (alkyl)(amino) carbenes (CAACs).

Solvent-dependent emission studies indicate that **1**–**4** have moderate intramolecular charge-transfer (ICT) behavior. Electrochemical investigations reveal that the NHO-containing boranes have extremely low reversible oxidation potentials (e.g., for **3**, $E_{1/2}^{ox} = -0.40$ V vs. ferrocene/ferrocenium, Fc/Fc$^+$, in THF). Time-dependent (TD) DFT calculations show that the HOMOs of **1**–**3** are much more destabilized than that of the enamine-containing **4**, which confirms the stronger donating ability of NHOs.

Introduction

Three-coordinate boron is sp^2 hybridized[1] and adopts a trigonal planar geometry, which leaves an unoccupied p-orbital. This vacant orbital can act as an excellent π-acceptor (A) in the excited state, leading to intramolecular charge transfer (ICT) after photoexcitation. As such, applications of three-coordinate boranes as selective anion sensors,[2] nonlinear optical (NLO) materials,[3] for two-photon absorption and two-photon excited fluorescence,[4] and live-cell imaging,[5] among others[6] have been intensively studied.

We are interested in designing small molecules (donor (D)–π–A type three-coordinate boranes) with narrow energy gaps. One approach is to stabilize the lowest unoccupied molecular
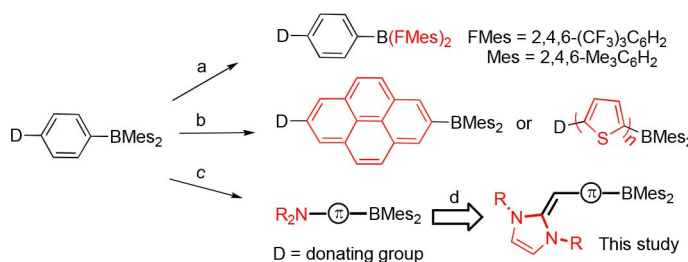
Scheme 1. Reported strategies to narrow the energy gap of boron containing D–π–A systems (a, b, c) and new systems reported in this study (d).

orbital (LUMO) by enhancement of the electron-acceptor strength of the boron center. Instead of using mesityls as steric protecting groups to avoid water or other nucleophiles binding to the empty orbital of boron,[7] Marder[8] and others[9] applied 2,4,6-(CF$_3$)$_3$C$_6$H$_2$ (FMes) as a new steric protecting group in three-coordinate boranes (Scheme 1a). A second approach is modification of the π-linker in D–π–A systems, for example, using pyrene[10] or thiophenes[3f,8e] (Scheme 1b), potentially influencing both the highest occupied molecular orbital (HOMO) and LUMO. The third method is to use a very electron-rich donor group which reduces the energy gap by destabilizing the HOMO (Scheme 1c). As an example, Marder, Braunschweig et al. have recently reported the use of a diborene (B≡B) system as the π-donor resulting in NIR absorbing and emitting quadrupolar systems,[11] but these compounds are rather unstable in air.

Amines are among the most efficient and well-studied π-electron donors in organic materials,[12] and triarylamines con-

[a] J. He, F. Rauch, Dr. A. Friedrich, Dr. D. Sieh, Dr. T. Ribbeck,
Dr. I. Krummenacher, Prof. Dr. H. Braunschweig, Prof. Dr. M. Finze,
Prof. Dr. T. B. Marder
Institute for Inorganic Chemistry and Institute for Sustainable Chemistry &
Catalysis with Boron (ICB), Julius-Maximilians-Universität Würzburg
Am Hubland, 97074 Würzburg (Germany)
E-mail: maik.finze@uni-wuerzburg.de
todd.marder@uni-wuerzburg.de

nected to triarylboranes were found to be suitable materials for OLEDs.[13] However, using two nitrogen atoms linked 1,1 to a C=C double bond, known as an N-heterocyclic olefin (NHO), as a donor (Scheme 1d), to the best of our knowledge, has never been combined with a three-coordinate borane acceptor.[14] NHOs are widely used as catalysts in transesterification, to turn CO_2 into valuable chemicals,[15] promote polymerization, etc.[16] Due to the donating effect of two nitrogen atoms, as well as the 6π-electrons of the imidazole ring, the exocyclic C=C bond becomes highly polarized and electron rich,[17] thus making NHOs potential strong donors.

With this in mind, we designed and synthesized four different boranes, 1–4 (Scheme 2), with 1–3 having an NHO as the donating group, whereas in 4, an enamine is the donating group. The two extra methyl groups in 2 versus 1 should improve the stability by protecting the exocyclic C=C bond. For a more efficient and π-electron-rich linker, borane 3 was designed. Herein, we report about the synthesis and properties of these new donor–π–acceptor three-coordinate boranes.
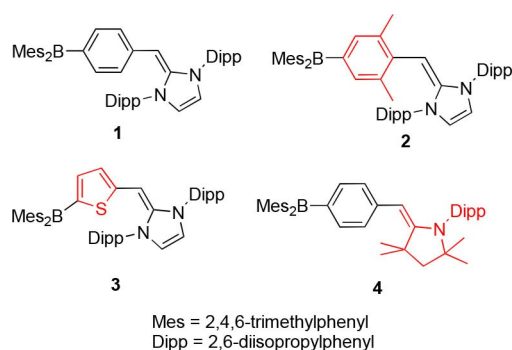
Scheme 2. Three-coordinate boranes 1–4 developed in this study.

Results and Discussion

Synthesis

The synthesis of the four boranes is shown in Scheme 3. Our strategy was to employ bromomethyl triaryl boranes 7a, 7b, 7c as precursors for the final step of the synthesis, namely the introduction of the NHO or enamine moiety. Thus, the corresponding silyl-protected brominated alcohols were treated with nBuLi at −78 °C, followed by the addition of FBMes₂, giving the intermediate boranes 6a, 6b, 6c in high yields. Subsequent consecutive treatment with PBr₃ and tetrabutylammonium bromide (TBAB) in CH₂Cl₂ at 0 °C, deprotection and bromination in one step, gave precursors in good (7a and 7b) to acceptable (7c) yields. TBAB is necessary in these reactions, otherwise the products are formed in much lower yields.[18] All compounds were fully characterized by NMR, high-resolution mass spectrometry (HRMS), as well as elemental analysis. Single crystals of 7a and 7b suitable for X-ray diffraction analysis were grown from dichloromethane/hexane at −30 °C and of 7c by evaporation of a hexane solution at room temperature. These precursors were then treated with 2 equiv of 1,3-bis-(2,6-diisopropylphenyl)imidazole-2-ylidene (IPr, for 7a, 7b and 7c) or 1-(2,6-diisopropylphenyl)-3,3,5,5-tetramethylpyrrolidine-2-ylidene (CAAC, for 7a), respectively, at room temperature. The solutions turned reddish-orange (for reactions with IPr) or yellow (for reaction with CAAC), immediately. After workup and crystallization, 1–4 were isolated in 90, 87, 85, and 45 % yields, respectively.

The identity and purity of 1–4 was confirmed by NMR spectroscopy, HRMS, and elemental analysis. The chemical shifts in the $^{11}B\{^1H\}$ NMR spectra are in the typical range of three-coordinate boranes ($\delta(^{11}B) = 69.6$, 71.9, 57.5, and 73.3 ppm for 1, 2, 3, and 4, respectively). Compound 3 has the highest field ^{11}B chemical shift which is attributed to the more efficient conjugation and donor ability of the thienyl group. In the ^1H NMR spectra, the signals of the protons of the exocyclic double bond appear at 4.00 (1), 3.69 (2), 4.38 (3), and 4.50 ppm (4). Another interesting observation is that the ^1H NMR spectra of 1 and 2 show broad signals in C_6D_6, but in CD_2Cl_2, all signals are sharp with well-resolved H–H couplings. In contrast, the ^1H NMR signals of 3 and 4 are well-resolved in both solvents, C_6D_6 and CD_2Cl_2.

Stability tests indicate that 1–3 decompose slowly in solution in air, so they have to be handled under an inert atmosphere. In stark contrast, compound 4 is a bench-stable yellow solid and shows no decomposition even in common solvents for several months, as evident from NMR spectroscopy.
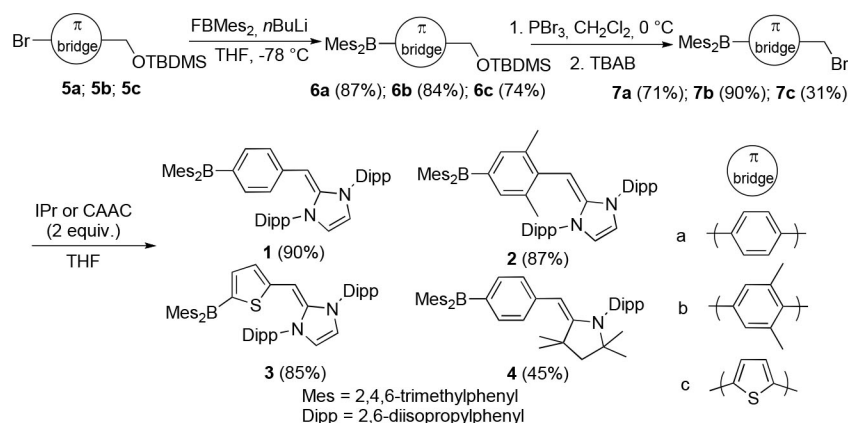
Scheme 3. Synthesis of three-coordinate boranes 1–4.
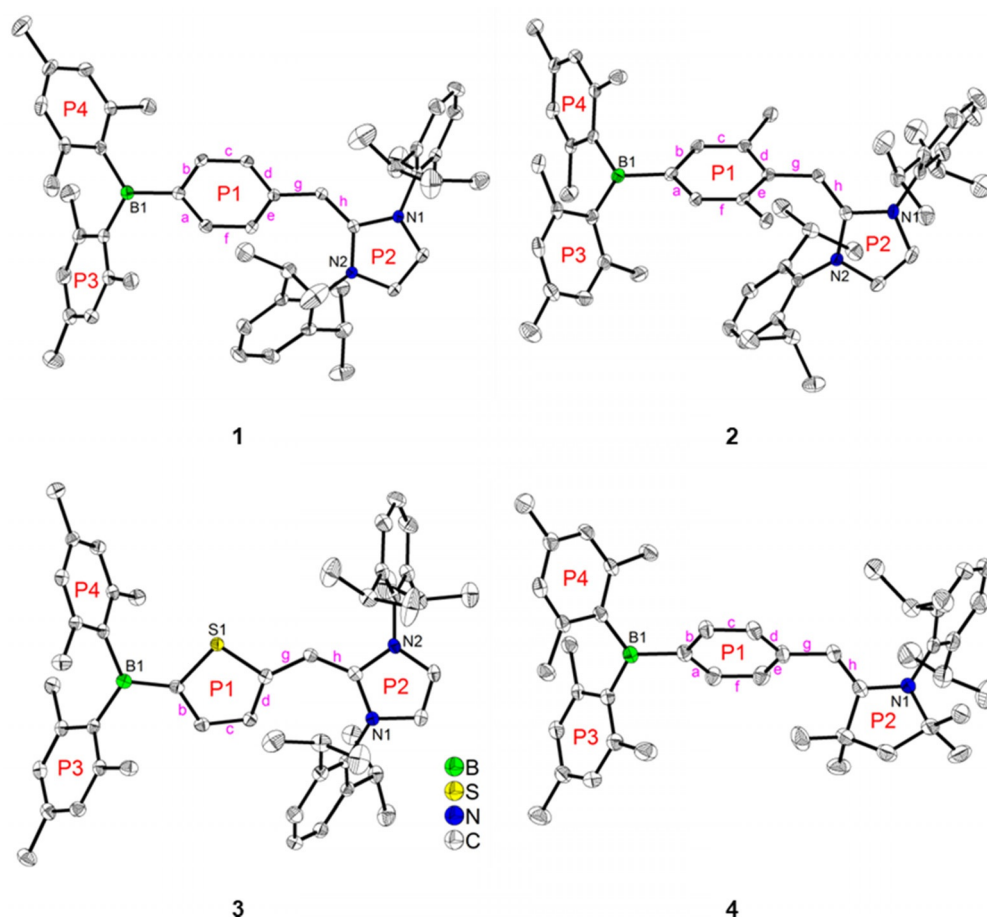
Figure 1. Molecular structures of **1**–**4** from single-crystal X-ray diffraction data at 100 K. Atomic displacement ellipsoids are drawn at the 50% probability level, and hydrogen atoms are omitted for clarity. For **4**, only one of two symmetrically independent molecules is shown. With regard to the aryl rings bonded to boron atoms, the central ring is labelled P1 and the terminal rings are labelled P3 and P4. The 5-membered nitrogen-containing ring is labelled P2. The pyrrolidine moiety of one of the two molecules of **4** is disordered, and only the part with 87% occupancy is shown.

Crystal structures

Reddish-orange single crystals suitable for X-ray diffraction analysis of **1** and **3** were grown by evaporation of a hexane solution at room temperature. Single crystals of **2** were obtained from a saturated acetonitrile solution and of **4** by crystallization from a dichloromethane/acetonitrile solution at −30 °C. The molecular structures in the solid state are shown in Figure 1 and selected bond lengths (Å) and interplanar angles

Table 1. Selected bond lengths [Å] and angles [°] of **1**–**4**.					
Compound	1	2	3	4 (molecule 1)[a]	4 (molecule 2)[a]
B1—C (P1)	1.547(2)	1.552(3)	1.512(3)	1.564(3)	1.558(3)
B1—C (P3)	1.581(2)	1.588(3)	1.586(3)	1.572(3)	1.572(3)
B1—C (P4)	1.583(2)	1.585(3)	1.583(3)	1.581(3)	1.584(3)
∡B1C₃-P1	17.69(7)	17.86(11)	11.72(10)	27.13(10)	29.13(10)
∡B1C₃-P3	56.72(6)	56.45(5)	58.10(8)	58.76(9)	58.07(9)
∡B1C₃-P4	60.31(6)	66.42(6)	61.13(8)	50.36(7)	50.56(7)
Sum ∡CB1C	359.9(1)	360.0(2)	360.0(2)	360.0(2)	360.0(2)
h (C=C)	1.379(2)	1.361(3)	1.382(3)	1.337(3)	1.334(3)
C—N1	1.388(2)	1.395(2)	1.376(2)	1.389(3)	–
C—N2	1.387(2)	1.407(2)	1.381(2)	–	1.392(3)
∡P1-P2	37.76(7)	57.74(7)	24.65(7)	83.89(9)	79.89(8)

With regard to the aryl rings bonded to boron atoms, the central ring is labelled P1 and the terminal rings are labelled P3 and P4. The 5-membered nitrogen containing ring is labelled P2. [a] In borane **4**, the boron and nitrogen atoms are labeled B1 and N1 in molecule 1 and B2 and N2 in molecule 2.

(°) are listed in Table 1. The three aryl groups attached to boron adopt propeller-like configurations in all four compounds. The BC$_3$ moieties are planar with the sum of the C-B-C bond angles equal to 360°. The interplanar angles between the BC$_3$ plane and the aryl groups bonded to boron depend on the steric demand of the aryl moieties. The terminal mesityl rings P3 and P4 are strongly twisted with respect to the BC$_3$ plane (50–66°, Table 1), a behavior that is generally observed in triarylboranes.[3g–i,4e,8c,e,19] The bridging aryl rings P1, which are sterically less demanding, are only slightly twisted with respect to the BC$_3$ plane (12–29°, Table 1). The B—C bond lengths lie in the expected range. They are longer to the mesityl groups (1.572(3)–1.588(3) Å), whereas they are significantly shorter to the bridging rings, that is, 1.547(2)–1.564(3) Å for the phenyl and xylyl rings (1, 2, and 4) and shortest at 1.512(3) Å for the thiophene group in 3 (Table 1). In 1–3 the exocyclic C=C double bond (h, Figure 1) length is significantly longer (1.361(3)–1.382(3) Å, Table 1) than a normal C=C double bond[20] or the exocyclic C=C bond of 1,3-bis(2,6-diisopropyl-phenyl)-2-methylene-2,3-dihydro-1H-imidazole (IPr=CH$_2$, 1.332(4) Å).[17] This suggests some degree of charge transfer in the ground state and a polarized ground state in 1–3. This is not the case for 4, in which h = 1.334(3) Å, close to the expected C=C double bond length. A pronounced bond-length alternation (0.036(3) Å, Table S3, Supporting Information) is observed for the phenyl and xylyl units of 1 and 2 consistent with a partially quinoidal structure. This indicates strong conjugation between the boron centers and the bridging units, which also suggests ground-state ICT. The bond-length alternation is less pronounced in 4 (0.018(3) Å). The interplanar angle between the bridging ring P1 and the N-heterocyclic carbene ring P2, which are connected through the exocyclic C=C double (h) and a C—C single bond (g), varies strongly among the compounds. Although these are smallest for 1 (38°) and 3 (25°), the angle is larger for 2 (58°), which has a sterically more demanding bridging ring, and largest for 4 (80° and 84°). Borane 4 has the largest dihedral angle between rings P1 and P2, probably due to less effective conjugation between the boron center and the bridging unit, which also is reflected by less bond length alternation of the bridge-phenyl group.

Electrochemical properties

To investigate their electrochemical properties, 1–4 were also studied by cyclic voltammetry (Table 2). Boranes 1–3 show both a reversible reduction wave and a reversible oxidation wave, whereas 4 reveals only a reversible reduction wave and a partially reversible oxidation wave (Figure 2). The reversible reduction waves are attributed to the BMes$_2$ moieties and the oxidation processes are related to the NHOs or the enamine moiety. The half-wave reduction potentials of 1 and 3 at −2.86 V are the most negative potentials among the four compounds. As expected, 4 ($E^{red}_{1/2} = -2.66$ V) has the most positive half-wave reduction potential. The half-wave reduction potential of 2 ($E^{red}_{1/2} = -2.82$ V) is 40 mV more positive than that for 1, which may be due to the larger dihedral angle between rings P1 and P2, as discussed above and the more rigid structure of

Table 2. Cyclic voltammetry data[a] for boranes 1–4.

	$E^{ox}_{1/2}$ [V]	$E^{red}_{1/2}$ [V]	HOMO [eV][c]	LUMO [eV][c]
1	−0.36	−2.86	−4.37	−2.00
2	−0.36	−2.82	−4.38	−2.05
3	−0.40	−2.86	−4.33	−2.00
4	0.27[b]	−2.66	−5.00	−2.20

[a] Measured in THF in the presence of 0.1 M nBu$_4$NPF$_6$, potential sweep rates of 250 mV s^{-1}, half-wave potentials are given against the Fc/Fc$^+$ couple. [b] Partially reversible half-wave oxidation potential. [c] Calculated from the onset potentials of the first oxidation and reduction waves, respectively, assuming that the HOMO of Fc lies 4.8 eV below the vacuum level.
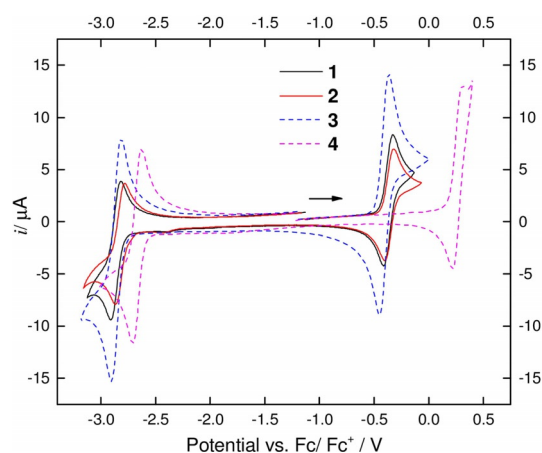
Figure 2. Cyclic voltammograms of 1(black, solid), 2 (red, solid), 3(blue, dash), and 4 (pink, dash).

2. The reversible reduction potentials of the NHO donor compounds are about 0.2 V more negative than that of the enamine donor compound. These reduction potentials are all comparable to those of other structurally related D–π–A boranes.[21] Obviously, the donor ability of the NHO or enamine unit does not have a large influence on the electron-accepting ability of the three-coordinate boron center in our compounds.

In sharp contrast to their very similar reduction potentials, large differences were found for their oxidation potentials depending on the donor moiety. Compounds 1 and 2 have the same half-wave oxidation potential (−0.36 V) and $E^{ox}_{1/2}$ of 3 (−0.40 V) is shifted to a more negative value by 40 mV, only. This small difference is caused by the more electron-rich thienyl bridge. Compounds 1–3 are easily oxidized and show far more negative oxidation potentials than 4 ($E^{ox}_{1/2} = 0.27$ V). This larger difference indicates that the NHO is far more electron rich than the enamine, and also suggests a much smaller HOMO–LUMO gap in NHO-containing 1–3 compared to enamine-containing 4. The comparably low reversible oxidation potentials of 1–3 are possibly the reason for their air-sensitivity (see above).

Table 3. Photophysical data for **1**–**4** at room temperature.

	Solvent	λ_{abs}[a] [nm] (ε [10^4 cm^{-1} M^{-1}])	λ_{em} [nm]	Φ_F[b]	τ_F [ns]	Stokes shift [cm^{-1}]
1	Hexane	485 (5.8)	499	[c]	[c]	578
	Toluene	495 (8.5)	528	0.15	2.1	1263
	THF	504 (7.4)	572	0.15	<1.0	2359
	Solid	–	576	0.11	1.9	–
2	Hexane	484 (3.0)	510	0.012	<1.0	1053
	Toluene	494 (3.4)	555	0.29	7.3	2225
	THF	501 (3.2)	649	0.033	1.6	4552
	Solid	–	569	0.074	[d]	–
3	Hexane	508 ([e])	525	(N.D.)[e]	[e]	638
	Toluene	516 ([e])	547	(N.D.)[e]	[e]	1098
	THF	522 ([e])	575	(N.D.)[e]	[e]	1766
	Solid	–	591	0.037	[d]	–
4	Hexane	411 (2.2)	432	[c]	<1.0	1183
	Toluene	421 (3.1)	454	0.005	<1.0	1727
	THF	421 (2.9)	475	0.012	<1.0	2700
	Acetonitrile	426 (3.6)	501	0.031	<1.0	3514
	Solid	–	467	0.003	<1.0	–

[a] Lowest-energy absorption maximum. [b] Absolute fluorescence quantum yields measured using an integrating sphere. [c] Not determined due to very weak emission. [d] **2**: $\tau_1 < 1.0$ (87.6%), $\tau_2 = 1.1$ (11.7%), $\tau_3 = 3.8$ ns (0.7%); Borane **3**: $\tau_1 < 1.0$ (87.7%), $\tau_2 = 1.9$ (12.2%), $\tau_3 = 11.2$ ns (0.1%). [e] Not determined due to slow decomposition in highly dilute solution.

Photophysical properties

UV–visible absorption spectra of **1**–**4** were measured in different solvents and the data are listed in Table 3. Compounds **1**–**4** have a strong, structureless lowest-energy absorption band in toluene with maxima at 495, 494, 516, and 421 nm, respectively (Figure 3), which can be attributed to ICT. The lowest-energy absorption of **4** in solution is similar to that of related D–π–BMes$_2$ compounds.[3i,4d] A comparison of the lowest-energy absorption bands shows a large red shift (e.g., in toluene, approx. 3500 cm^{-1} for **1** and **2**, 4300 cm^{-1} for **3**) between NHO-containing **1**–**3** and enamine-containing **4**, indicating the stronger π-electron donating ability of the NHO than the enamine. The redshift of about 20 nm (860 cm^{-1}) observed for **3** compared to **1** confirms the more efficient conjugation of a thienyl compared with a phenyl group, which was discussed for the electrochemical data (see above). Another interesting finding is that **1** has a very large molar extinction coefficient (8.5×10^4 cm^{-1} M^{-1} in toluene and 7.4×10^4 cm^{-1} M^{-1} in THF) for the lowest-energy absorption. With increasing solvent polarity, positive absorption solvatochromism (approx. 15 nm from hexane to THF) was observed in all four boranes, which suggests polarized ground states and moderate ground-state dipole moments,[3i,22] caused by ground-state ICT.
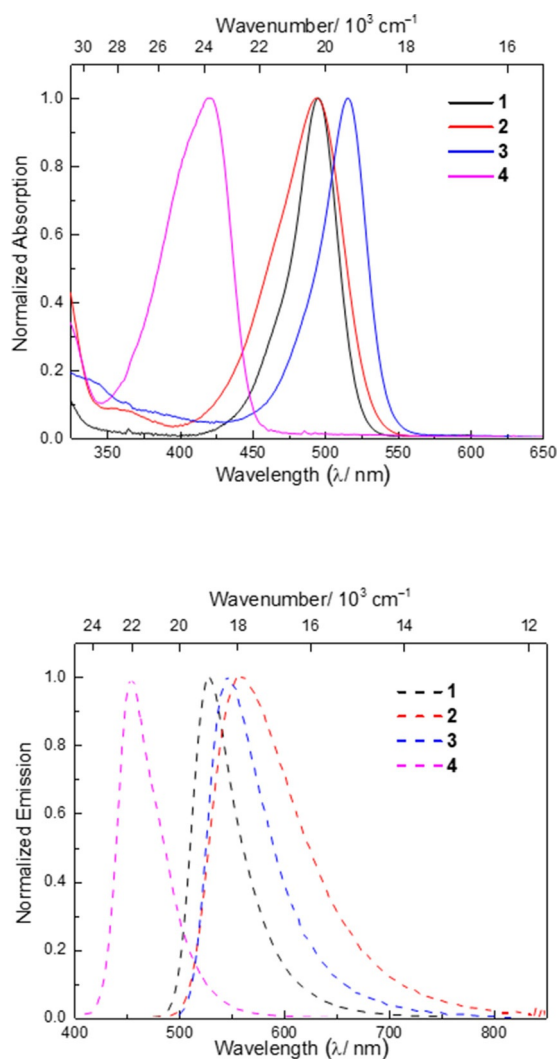
All of the boranes show weak to moderate emission in solution and in the solid state. Solvent-dependent emission studies indicate that all of the boranes show a moderate redshift with increasing solvent polarity. This is a typical phenomenon observed in D–π–A compounds due to ICT, resulting in a more polarized excited state, which is stabilized by a higher-polarity solvent relative to the ground state. The Stokes shifts of the boranes also increase with increasing solvent polarity. In THF, **2**

has the largest Stokes shift (4552 cm^{-1}) among all four boranes in different solvents. In the solid state, **1** exhibits the highest quantum yield (0.11) and **3** has the lowest-energy emission (591 nm) but with a much lower quantum yield (0.037). It was not possible to determine the molar extinction coefficient, quantum yield and life-time of **3** in solution accurately due to slow decomposition in highly dilute solution.

Theoretical studies

DFT calculations were carried out to gain deeper insight into the electronic and photophysical properties of **1**–**4**. Optimized ground-state structures were obtained at the B3LYP/6–31+G(d) level of theory using the crystal structures as the starting geometries. The solid-state structures were nicely reproduced. Similar to the crystal structures, the mesityl C–B bonds are about 0.04 (**1**), 0.03 (**2**), 0.06 (**3**), and 0.03 Å (**4**) longer than the π-bridge B–C bonds. In comparison with experimental values, the angles between the BC$_3$ plane and the π-bridge are slightly larger for **1**–**3** ($\Delta = 3.90°$, 0.71° and 2.32° respectively) and smaller for **4** ($\Delta = 4.12°$ and 6.13°). The optimized structures also exhibit a quinoidal distortion of the π-bridge. The mean quinoidal distortions of the phenylene-bridged compounds **1** and **4** are 0.03 and 0.026 Å, respectively. In the xylene-bridged derivative **2**, it is not sensible to use the mean distortion because the methyl groups on the donor side also influence the aromatic bond lengths. In this case, the bonds a/b are 0.02 Å longer than c/f, whereas e/d are 0.03 Å longer (Figure 1). In the thiophene-bridged **3**, all bond lengths are similar to those in the crystal structure.

The optimized structures also reproduce the shortened C–C single bond (g) and the elongated exocyclic C=C double bond

HOMOs of **1**–**3** are very similar in energy ($\Delta E < 0.05$ eV), as are the LUMOs, which indicates only a small influence of the different bridges on the frontier orbitals. Borane **4**, however, exhibits a lower HOMO as well as LUMO energy ($\Delta E = 0.5$ and 0.2 eV, respectively, in comparison to **1**), which nicely fits with the electrochemical study. This is due to the significantly lower donor strength of the enamine than the NHO.

Table 4. Lowest-energy transitions calculated at the B3LYP/6–31 + G(d) level of theory. (H = HOMO; L = LUMO).

Compound	Transition	E [eV]	λ [nm]	f	Major contributions	Λ	Dipole moment [D]
1	$S_1 \leftarrow S_0$	2.63	471	0.59	H→L (98%)	0.54	6.27
2	$S_1 \leftarrow S_0$	2.56	484	0.36	H→L (99%)	0.46	5.53
3	$S_1 \leftarrow S_0$	2.65	467	0.62	H→L (98%)	0.64	7.03
4	$S_1 \leftarrow S_0$	2.99	415	0.75	H→L (98%)	0.56	6.26

Subsequently, TD-DFT calculations were carried out at the B3LYP/6–31+G(d) level of theory. In the gas phase, the $S_1 \leftarrow S_0$ transitions of all four derivatives are almost exclusively HOMO-to-LUMO transitions (Table 4). For ICT-based transitions it is recommended to use the Coulomb attenuated functional CAM-B3LYP.[23] We have carried out these calculations as well (see the Supporting Information). However, the calculations performed using B3LYP more accurately reproduced the energies found experimentally. Given that this was unexpected, we further determined the overlap coefficients (Λ) (Table 4).[24] Compounds **1**–**4** exhibit Λ coefficients around 0.5 for their lowest-energy transitions, which indicates only moderate ICT character in the excited state. For this reason, the B3LYP functional was used for the TD-DFT calculations as well.

This moderate ICT character of the lowest-energy absorptions could be due to an already partially polarized ground

Figure 3. UV–visible absorption (top) and emission spectra (bottom) of boranes **1**–**4** in toluene.

(h) that connects the donor to the bridge for **1**–**3**. In **4**, this convergence is more pronounced than in the crystal structure. This might be due to a significantly smaller angle between the P1 and P2 rings (33.55° vs. 80/84°) in **1**–**3**. This would lead to an increased interaction between the donor and acceptor which is most likely responsible for the changes in these bond lengths.

For **1**–**3**, the HOMO is mainly delocalized over the π-bridge, the exocyclic C=C double bond, and the imidazole ring (Figure 4). For **4**, the HOMO is mainly delocalized over the π-bridge, the exocyclic C=C double bond, and the nitrogen of the pyrrolidine ring. Interestingly, the boron also contributes to the HOMO in all compounds confirming the ground-state ICT. In all compounds, the LUMO is mainly localized on boron and the π-bridge, with the two mesityl groups and the exocyclic C=C double bond also contributing to some extent, along with a small contribution from the imidazole or pyrrolidine ring. The
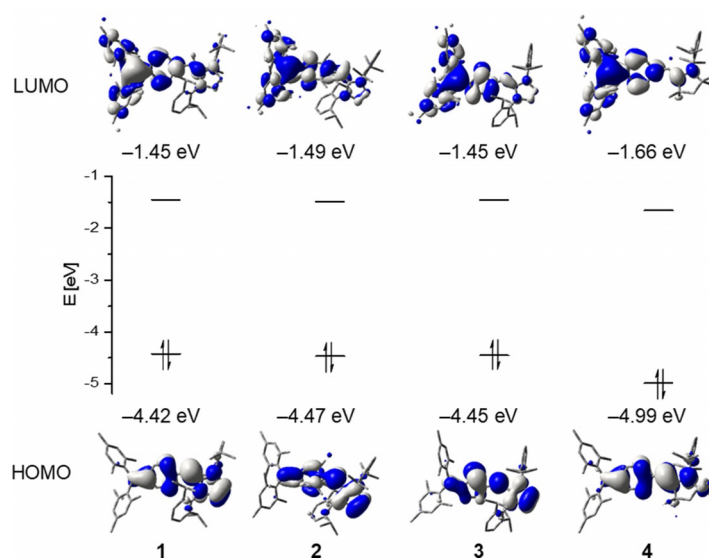

Figure 4. HOMO and LUMO of **1**–**4**, calculated at the B3LYP/6–31 + G(d) level of theory and corresponding energies.

state, which would decrease the change in dipole moment and necessity for solvent rearrangement upon excitation. All calculated structures exhibit moderate dipole moments in the ground state (Table 4), which also supports that assumption. The moderate positive absorption solvatochromism of all compounds with increasing solvent polarity also confirms the moderate ground-state dipole moments.

Conclusions

Four different D–π–A boranes were synthesized in three steps each, providing an efficient synthetic strategy for introducing N-heterocyclic olefins (NHO) into boron-containing D–π–A systems. Photophysical studies show that NHO is a much stronger electron donor than an enamine (or amine). The electrochemical investigations reveal extremely low reversible oxidation potentials for the three NHO-containing boranes **1**–**3** compared with those of enamine- (**4**) or amine-containing boranes. DFT calculations indicate a much higher HOMO for **1**–**3** in agreement with the strong electron-donating ability of the NHO moiety. Our studies confirmed the electron-rich property of NHOs, suggesting their potential for use as donors in other push–pull systems. The reversible oxidation potentials of **1**–**3** suggest that radical cations may be isolable, which is currently under investigation.

Acknowledgements

Conflict of interest

The authors declare no conflict of interest.

Keywords: donor–acceptor systems · electrochemistry · N-heterocyclic olefins · photophysical properties · triarylboranes

[1] H. C. Brown, V. H. Dodson, *J. Am. Chem. Soc.* **1957**, *79*, 2302–2306.

[2] a) T. W. Hudnall, C.-W. Chiu, F. P. Gabbaï, *Acc. Chem. Res.* **2009**, *42*, 388–397; b) C. R. Wade, A. E. J. Broomsgrove, S. Aldridge, F. P. Gabbaï, *Chem. Rev.* **2010**, *110*, 3958–3984; c) F. Jäkle, *Chem. Rev.* **2010**, *110*, 3985–4022; d) Z. M. Hudson, S. Wang, *Acc. Chem. Res.* **2009**, *42*, 1584–1596.

[3] a) Z. Yuan, N. J. Taylor, T. B. Marder, I. D. Williams, S. K. Kurtz, L.-T. Cheng, *J. Chem. Soc. Chem. Commun.* **1990**, *21*, 1489–1492; b) M. Lequan, R. M. Lequan, K. C. Ching, *J. Mater. Chem.* **1991**, *1*, 997–999; c) M. Lequan, R. M. Lequan, K. C. Ching, M. Barzoukas, A. Fort, H. Lahoucine, G. Bravic, D. Chasseau, J. Gaultier, *J. Mater. Chem.* **1992**, *2*, 719–725; d) M. Lequan, R. M. Lequan, K. Chane-Ching, A.-C. Callier, M. Barzoukas, A. Fort, *Adv. Mater. Opt. Electron.* **1992**, *1*, 243–247; e) Z. Yuan, N. J. Taylor, Y. Sun, T. B. Marder, I. D. Williams, L.-T. Cheng, *J. Organomet. Chem.* **1993**, *449*, 27–37; f) C. Branger, M. Lequan, R. M. Lequan, M. Barzoukas, A. Fort, *J. Mater. Chem.* **1996**, *6*, 555–558; g) Z. Yuan, N. J. Taylor, R. Ramachandran, T. B. Marder, *Appl. Organomet. Chem.* **1996**, *10*, 305–316; h) Z. Yuan, J. C. Collings, N. J. Taylor, T. B. Marder, C. Jardin, J.-F. Halet, *J. Solid State Chem.* **2000**, *154*, 5–12; i) Z. Yuan, C. D. Entwistle, J. C. Collings, D. A. Jové, A. S. Batsanov, J. A. K. Howard, N. J. Taylor, H. M. Kaiser, D. E. Kaufmann, S. Y. Poon, W. Y. Wong, C. Jardin, S. Fathallah, A. Boucekkine, J. F. Halet, T. B. Marder, *Chem. Eur. J.* **2006**, *12*, 2758–2771.

[4] a) Z.-Q. Liu, Q. Fang, D. Wang, G. Xue, W.-T. Yu, Z.-S. Shao, M.-h. Jiang, *Chem. Commun.* **2002**, *23*, 2900–2901; b) Z.-Q. Liu, Q. Fang, D. Wang, D.-X. Cao, G. Xue, W.-T. Yu, H. Lei, *Chem. Eur. J.* **2003**, *9*, 5074–5084; c) M. Charlot, L. Porrès, C. D. Entwistle, A. Beeby, T. B. Marder, M. Blanchard-Desce, *Phys. Chem. Chem. Phys.* **2005**, *7*, 600–606; d) J. C. Collings, S.-Y. Poon, C. L. Droumaguet, M. Charlot, C. Katan, L.-O. Pålsson, A. Beeby, J. A. Mosely, H. M. Kaiser, D. Kaufmann, W.-Y. Wong, M. Blanchard-Desce, T. B. Marder, *Chem. Eur. J.* **2009**, *15*, 198–208; e) L. Ji, R. M. Edkins, L. J. Sewell, A. Beeby, A. S. Batsanov, K. Fucke, M. Drafz, J. A. K. Howard, O. Moutounet, F. Ibersiene, A. Boucekkine, E. Furet, Z. Liu, J.-F. Halet, C. Katan, T. B. Marder, *Chem. Eur. J.* **2014**, *20*, 13618–13635.

[5] a) S. Griesbeck, Z. Zhang, M. Gutmann, T. Lühmann, R. M. Edkins, G. Clermont, A. N. Lazar, M. Haehnel, K. Edkins, A. Eichhorn, M. Blanchard-Desce, L. Meinel, T. B. Marder, *Chem. Eur. J.* **2016**, *22*, 14701–14706; b) S. Griesbeck, M. Ferger, C. Czernetzki, C. G. Wang, R. Bertermann, A. Friedrich, M. Haehnel, D. Sieh, M. Taki, S. Yamaguchi, T. B. Marder, *Chem. Eur. J.* **2019**, *25*, 7679–7688; c) S. Griesbeck, E. Michail, C. G. Wang, H. Ogasawara, S. Lorenzen, L. Gerstner, T. Zang, J. Nitsch, Y. Sato, R. Bertermann, M. Taki, C. Lambert, S. Yamaguchi, T. B. Marder, *Chem. Sci.* **2019**, *10*, 5405–5422.

[6] For reviews, see: a) C. D. Entwistle, T. B. Marder, *Angew. Chem. Int. Ed.* **2002**, *41*, 2927–2931; *Angew. Chem.* **2002**, *114*, 3051–3056; b) C. D. Entwistle, T. B. Marder, *Chem. Mater.* **2004**, *16*, 4574–4585; c) S. Yamaguchi, A. Wakamiya, *Pure Appl. Chem.* **2006**, *78*, 1413–1424; d) F. Jäkle, *Coord. Chem. Rev.* **2006**, *250*, 1107–1121; e) Y. Ren, F. Jäkle, *Dalton Trans.* **2016**, *45*, 13996–14007; f) L. Ji, S. Griesbeck, T. B. Marder, *Chem. Sci.* **2017**, *8*, 846–863; g) S.-Y. Li, Z.-B. Sun, C.-H. Zhao, *Inorg. Chem.* **2017**, *56*, 8705–8717.

[7] J. Doty, B. Babb, P. Grisdale, M. Glogowski, J. Williams, *J. Organomet. Chem.* **1972**, *38*, 229–236.

[8] a) S. M. Cornet, K. B. Dillon, C. D. Entwistle, M. A. Fox, A. E. Goeta, H. P. Goodwin, T. B. Marder, A. L. Thompson, *Dalton Trans.* **2003**, *23*, 4395–4405; b) X. Yin, J. Chen, R. A. Lalancette, T. B. Marder, F. Jäkle, *Angew. Chem. Int. Ed.* **2014**, *53*, 9761–9765; *Angew. Chem.* **2014**, *126*, 9919–9923; c) Z. Zhang, R. M. Edkins, J. Nitsch, K. Fucke, A. Steffen, L. E. Longobardi, D. W. Stephan, C. Lambert, T. B. Marder, *Chem. Sci.* **2015**, *6*, 308–321; d) Z. Zhang, R. M. Edkins, M. Haehnel, M. Wehner, A. Eichhorn, L. Mailänder, M. Meier, J. Brand, F. Brede, K. M. Buschbaum, H. Braunschweig, T. B. Marder, *Chem. Sci.* **2015**, *6*, 5922–5927; e) Z. Zhang, R. M. Edkins, J. Nitsch, K. Fucke, A. Eichhorn, A. Steffen, Y. Wang, T. B. Marder, *Chem. Eur. J.* **2015**, *21*, 177–190.

[9] a) V. C. Gibson, C. Redshaw, W. Clegg, M. R. J. Elsegood, *Polyhedron* **1997**, *16*, 2637–2641; b) C. Redshaw, M. R. J. Elsegood, *Chem. Commun.* **2005**, *40*, 5056–5058; c) W. Fraenk, T. M. Klapötke, B. Krumm, P. Mayer, H. Nöth, H. Piotrowski, M. Suter, *J. Fluor. Chem.* **2001**, *112*, 73–81; d) A. E. J. Broomsgrove, D. A. Addy, A. D. Paolo, I. R. Morgan, C. Bresner, V. Chislett, I. A. Fallis, A. L. Thompson, D. Vidovic, S. Aldridge, *Inorg. Chem.* **2010**, *49*, 157–173; e) J. Wang, Y. Wang, T. Taniguchi, S. Yamaguchi, S. Irle, *J. Phys. Chem. A* **2012**, *116*, 1151–1158; f) T. Taniguchi, J. Wang, S. Irle, S. Yamaguchi, *Dalton Trans.* **2013**, *42*, 620–624; g) M. F. Smith, S. J. Cassidy, I. A. Adams, M. Vasiliu, D. L. Gerlach, D. A. Dixon, P. A. Rupar, *Organometallics* **2016**, *35*, 3182–3191; h) X. Yin, F. Guo, R. A. Lalancette, F. Jäkle, *Macromolecules* **2016**, *49*, 537–546; i) D. T. Yang, S. K. Mellerup, J. B. Peng, X. Wang, Q. S. Li, S. Wang, *J. Am. Chem. Soc.* **2016**, *138*, 11513–11516; j) X. Yin, K. Liu, Y. Ren, R. A. Lalancette, Y. L. Loo, F. Jäkle, *Chem. Sci.* **2017**, *8*, 5497–5505.

[10] a) S. B. Zhao, P. Wucher, Z. M. Hudson, T. M. McCormick, X. Y. Liu, S. N. Wang, X. D. Feng, Z. H. Lu, *Organometallics* **2008**, *27*, 6446–6456; b) A. G. Crawford, A. D. Dwyer, Z. Q. Liu, A. Steffen, A. Beeby, L.-O. Pålsson, D. J. Tozer, T. B. Marder, *J. Am. Chem. Soc.* **2011**, *133*, 13349–13362; c) A. Crawford, Z. Q. Liu, I. A. I. Mkhalid, M. H. Thibault, N. Schwarz, G. Alcaraz, A. Steffen, J. C. Collings, A. S. Batsanov, J. A. K. Howard, T. B. Marder, *Chem. Eur. J.* **2012**, *18*, 5022–5035; d) L. Ji, R. M. Edkins, A. Lorbach, I. Krummenacher, C. Brückner, A. Eichhorn, H. Braunschweig, B.

Engels, P. J. Low, T. B. Marder, *J. Am. Chem. Soc.* **2015**, *137*, 6750–6753; e) R. Kurata, A. Ito, M. Gon, K. Tanaka, Y. Chujo, *J. Org. Chem.* **2017**, *82*, 5111–5121; f) J. Merz, J. Fink, A. Friedrich, I. Krummenacher, H. H. A. Mamari, S. Lorenzen, M. Haehnel, A. Eichhorn, M. Moos, M. Holzapfel, H. Braunschweig, C. Lambert, A. Steffen, L. Ji, T. B. Marder, *Chem. Eur. J.* **2017**, *23*, 13164–13180; g) N. N. Yuan, W. Q. Wang, Y. Fang, J. C. Zuo, Y. Zhao, G. W. Tan, X. P. Wang, *Organometallics* **2017**, *36*, 2498–2501; h) L. Ji, I. Krummenacher, A. Friedrich, A. Lorbach, M. Haehne, K. Edkins, H. Braunschweig, T. B. Marder, *J. Org. Chem.* **2018**, *83*, 3599–3606.

[11] T. E. Stennett, P. Bissinger, S. Griesbeck, S. Ullrich, I. Krummenacher, M. Auth, A. Sperlich, M. Stolte, K. Radack, C.-J. Yao, F. Würthner, A. Steffen, T. B. Marder, H. Braunschweig, *Angew. Chem. Int. Ed.* **2019**, *58*, 6449–6454; *Angew. Chem.* **2019**, *131*, 6516–6521.

[12] O. Kwon, S. Barlow, S. A. Odom, L. Beverina, N. J. Thompson, E. Zojer, J. L. Brédas, S. R. Marder, *J. Phys. Chem. A* **2005**, *109*, 9346–9352.

[13] a) Y. Shirota, M. Kinoshita, T. Noda, K. Okumoto, T. Ohara, *J. Am. Chem. Soc.* **2000**, *122*, 11021–11022; b) H. Doi, M. Kinoshita, K. Okumoto, Y. Shirota, *Chem. Mater.* **2003**, *15*, 1080–1089; c) D. Mutaguchi, K. Okumoto, Y. Ohsedo, K. Moriwaki, Y. Shirota, *Org. Electron.* **2003**, *4*, 49–59; d) W. L. Jia, D. R. Bai, T. McCormick, Q. D. Liu, M. Motala, R. Y. Wang, C. Seward, Y. Tao, S. Wang, *Chem. Eur. J.* **2004**, *10*, 994–1006; e) W. L. Jia, X. D. Feng, D. R. Bai, Z. H. Lu, S. Wang, G. Vamvounis, *Chem. Mater.* **2005**, *17*, 164–170; f) W. L. Jia, M. J. Moran, Y. Y. Yuan, Z. H. Lu, S. Wang, *J. Mater. Chem.* **2005**, *15*, 3326–3333; g) F. Li, W. Jia, S. Wang, Y. Zhao, Z. H. Lu, *J. Appl. Phys.* **2008**, *103*, 034509; h) Z. Chen, X. K. Liu, C. J. Zheng, J. Ye, C. L. Liu, F. Li, X. M. Ou, C. S. Lee, X. H. Zhang, *Chem. Mater.* **2015**, *27*, 5206–5211.

[14] a) C. E. I. Knappke, A. J. Arduengo, H. J. Jiao, J. M. Neudörfl, A. J. V. Wangelin, *Synthesis* **2011**, *23*, 3784–3795; b) R. Bertermann, H. Braunschweig, C. K. L. Brown, A. Damme, R. D. Dewhurst, C. Hörl, T. Kramer, I.

[15] Y. B. Wang, Y. M. Wang, W. Z. Zhang, X. B. Lu, *J. Am. Chem. Soc.* **2013**, *135*, 11996–12003.

[16] a) R. D. Crocker, T. V. Nguyen, *Chem. Eur. J.* **2016**, *22*, 2208–2213; b) M. M. D. Roy, E. Rivard, *Acc. Chem. Res.* **2017**, *50*, 2017–2025.

[17] S. M. Ibrahim Al-Rafia, A. C. Malcolm, S. K. Liew, M. J. Ferguson, R. McDonald, E. Rivard, *Chem. Commun.* **2011**, *47*, 6987–6989.

[18] A. Franzke, A. Pfaltz, *Synthesis* **2008**, *2*, 245–252.

[19] L. Weber, D. Eickhoff, T. B. Marder, M. A. Fox, P. J. Low, A. D. Dwyer, D. J. Tozer, S. Schwedler, A. Brockhinke, H.-G. Stammler, B. Neumann, *Chem. Eur. J.* **2012**, *18*, 1369–1382.

[20] F. H. Allen, O. Kennard, D. G. Watson, *J. Chem. Soc. Perkin Trans. 2* **1987**, S1–S19.

[21] a) R. Stahl, C. Lambert, C. Kaiser, R. Wortmann, R. Jakober, *Chem. Eur. J.* **2006**, *12*, 2358–2370; b) A. Ito, K. Kawanishi, E. Sakuda, N. Kitamura, *Chem. Eur. J.* **2014**, *20*, 3940–3953.

[22] Z. Yuan, N. J. Taylor, T. B. Marder, I. D. Williams, S. K. Kurtz, L. T. Cheng in *Organic Materials for Non-linear Optics II* (Eds.: R. A. Hann, D. Bloor), The Royal Society of Chemistry, Cambridge, **1991**, pp. 190–196.

[23] T. Yanai, D. P. Tew, N. C. Handy, *Chem. Phys. Lett.* **2004**, *393*, 51–57.

[24] M. J. G. Peach, P. Benfield, T. Helgaker, D. J. Tozer, *J. Chem. Phys.* **2008**, *128*, 044118.

Krummenacher, B. Pfaffinger, K. Radacki, *Chem. Commun.* **2014**, *50*, 97–99; c) C. J. Berger, G. He, C. Merten, R. McDonald, M. J. Ferguson, E. Rivard, *Inorg. Chem.* **2014**, *53*, 1475–1486.